The production of rice straw-derived biochar and its application for enhanced decolorization of azo dye as the role of redox mediator

Cong Ding[a], Jingjing Yang[b], Tianyin Huang[a],*, Wei Wu[a], Liming Zhang[a], Wenjun Xia[a], Jiabin Chen[c],*

[a]*School of Environmental Science and Engineering, Suzhou University of Science and Technology, Suzhou 215006, China,*
Tel. +13962512379; email: huangtianyin111@163.com (T. Huang), Tel. +15720887541; email: dc2475962@163.com (C. Ding),
Tel. +18662600395; emails: wuwei@usts.edu.cn (W. Wu), 695569932@qq.com (L. Zhang), Tel. +15190074300;
email: 695569932@qq.com (W. Xia)
[b]*Center for Separation and Purification Materials and Technologies, Suzhou University of Science and Technology, Suzhou 215009,*
China, email: yjjnancy@163.com (J. Yang)
[c]*State Key Laboratory of Pollution Control and Resources Reuse, College of Environmental Science and Engineering,*
Tongji University, Shanghai 200092, China, Tel. +13962512601; email: chenjiabincn@163.com (J. Chen)

ABSTRACT

The rice straw biochar (RSB) was prepared from rice straw by chemical/thermal treatment, and then characterized by scanning electron microscopy, Brunauer–Emmett–Teller, Fourier transform infrared spectroscopy, and Raman spectra. RSB was used to enhance the chemical or biological decolorization of an azo dye, orange G (OG), to evaluate the redox mediator property. Results showed that RSB could significantly accelerate the chemical reduction of OG with Na_2S as the electron donor. Such an accelerating effect was positively related to RSB loading, Na_2S concentration, and temperature, but negatively related to pH. In the anaerobic biological decolorization of OG, the addition of RSB could enhance the decolorization rate from 53.7% to 83.5% after 48 h. The synergistic effect of RSB on the biological decolorization of OG could be attributed to the role of redox mediator of the oxygen group on the surface of RSB, which could accelerate the electrons transfer from substrate to azo bond. The functioning of RSB as a redox mediator to enhance the decolorization rate was further verified in a continuous flow up-flow anaerobic sludge blanket reactor. Finally, the decolorization products of OG were analyzed by UV-vis and gas-chromatography and mass spectrometry, and the mechanism was subsequently proposed.

Keywords: Azo dye; Rice straw; Biochar; Redox mediator; Decolorization; Pathway

1. Introduction

Due to the wide use of azo dyes in various industries, the adverse impact of azo dye wastewaters on the environment has attracted considerable attention [1]. Biological methods are commonly used to treat azo dye wastewater and have the advantages of low-cost, easy-operation, and low-environmental impact. However, they also have the disadvantage of low decolorization rates, long hydraulic retention time (HRT) in the biological treatment [2]. Electron transfer is one of the rate-limiting steps in the cleavage of azo bonds in biological treatment [3]. How to accelerate the electron transfer is crucial for enhancing the biological decolorization efficiency of azo dyes. The addition of redox mediators (RM) to improve the efficiency of anaerobic

* Corresponding authors.

biological treatment has received great attention. For example, anthraquinone disulfonate and anthraquinone-2,6-disulfonic are effective RM to enhance the decolorization of azo dyes [4]. However, the homogenous RM is easy to drain away and hard to be recovered, which may produce waste or secondary environmental pollution [5]. Recently, the carbon materials such as activated carbon (AC), carbon nanotubes, and graphene oxide have been used as heterogeneous RM to enhance the decolorization of azo dyes, owing to the abundant functional groups possessing electron shuttling property on the surface [6–12].

Activated carbon (AC) is a kind of adsorbent and catalyst with a wide range of uses. Due to the high cost of preparation, the utilization of AC is limited. In recent years, researchers at home and abroad have focused on how to use low-cost and high carbon content agricultural waste to prepare AC, so that the cost can also be greatly reduced when obtaining high specific surface area AC products [13]. Waste in the form of agricultural by-products is a widespread problem. At present, the total annual yield of rice straw in China is more than 800 million tons [14], which if fully utilized, will be an abundant agricultural biomass resource. Researches have shown that there are large quantities of cellulose, hemicellulose, and lignin in rice straw [15]. However, each year, large quantities of rice straw remain unused and are burned. Biochar is a kind of carbonaceous substance produced by slow pyrolysis of biomass at low temperature (usually below 700°C) under anoxic condition [16]. Thus, if modified reasonably, rice straw will be a potential environmental functional material to excellently functional biochar.

In fact, because of its rich raw materials and excellent structure, more and more researchers begin to study straw biochar. Containing a large proportion of active hydroxyl groups, endows it with good adsorption properties for inorganic ions, organic compounds, and metals [15]. Rocha et al. [16] used triturated rice straw treated with NaOH solution as a biosorben and demonstrated its ability in the removal of metal ions such as Cu(II), Zn(II), Cd(II), and Hg(II). Daifullah et al. [17] found that $KMnO_4^-$ modified rice straw biochar (RSB) was potentially suitable as an adsorbent for fluoride anions in aqueous solutions. Mantell [18] found activated biochar made from soft, lower density precursors, such as rice hulls, a good adsorbent. Besides, RSB is a versatile catalyst support due to its chemical stability, biocompatibility, and high specific surface area and pore volume distribution [19]. Oh and Seo [20] investigated that Co-pyrolysis of polymer and rice straw increased the carbon content, cation exchange capacity, surface area and pH of the biochar and enhance the sorption of 2,4-dinitrotoluene and Pb. The importance of surface functional groups and the aromaticity of polymer/RS-derived biochar as an electron transfer mediator are being investigated. Yu et al. [21] indicated that RSB significantly accelerate electron transfer from cells to PCP, thus enhancing reductive dechlorination.

Thus, the objectives to this work is (1) to prepare a resource-friendly biochar with high specific surface and good adsorption and catalytic performance with the waste RSB and (2) to identify its effect to enhance the decolorization of orange G (OG) as a redox mediator. The role of redox mediator of RSB was evaluated both in accelerating the chemical reduction of OG with Na_2S as the electron donor and enhancing biological decolorization of OG by anaerobic granular sludge (AGS). Finally, a bench-scale test in continuous flow upflow anaerobic sludge blanket (UASB) reactor was carried out to prepare for the future of industrialization.

2. Materials and methods

2.1. Chemicals

Sources of chemicals are provided in Table 1. All chemicals were used as received without further purification. Purified water was used was used for washing and experiments.

2.2. Preparation of RSB

The straw used in the study was collected from local farmland in southeastern China. Dried rice straws were firstly cut into 5 cm lengths and immersed in the impregnation liquid with 2 wt.% NaOH for 48 h to remove ash, wax, and water-soluble impurities on the surface of the material. They were then washed with distilled water until neutral and dried at 105°C in an oven for later use. Samples of 20 g were placed in four beakers numbered 1–4, containing 300 mL impregnation liquid with 0, 10, 20, and 30 wt.% $(NH_4)_2HPO_4$ respectively, for 24 h and then dried at 105°C in an oven (numbered as RSB_0, RSB_1, RSB_2, and RSB_3, respectively). The samples were then pre-oxidized in an electrothermostatic blast oven at 200°C for 2 h. Finally, they were pyrolyzed in a box-type atmosphere furnace under nitrogen flow with the following protocol: heating from room temperature to 500°C at a rate of 25°C min^{-1}, then heating to 700°C at a rate of 13°C min^{-1}, and maintaining at 700°C for 60 min. After cooling to room temperature, the samples were ground and passed through a 100 mesh sieve.

2.3. Characterization of RSB

The morphological analysis of RSB was conducted by scanning electron microscopy (SEM, Quanta 250, FEI, USA), operating at an accelerating voltage of 10 kV. The specific surface area of RSB was obtained by the Brunauer–Emmett–Teller method (BET, ASAP 2020, Micromeritics, USA). The functional groups in RSB were analyzed by Fourier transform infrared spectroscopy (FT-IR, Nicolet 6700, Thermo Fisher Scientific, USA) in the range 500 to 4,000 cm^{-1}. Raman analysis was conducted on a Raman spectrometer DXR (DXR SmartRaman, Thermo Fisher Scientific, USA).

2.4. Chemical decolorization of OG

The prepared material, RSB, was tested as RM on the chemical decolorization of OG (1 mg L^{-1}). OG decolorization by Na_2S was monitored in the presence and absence of RSB. The experiments were performed in triplicate. RSB was added to 100 mL glass serum bottles. The flasks were sealed with butyl rubber stoppers, and the gas headspace was flushed for 2 min with N_2. Buffer with Na_2HPO_4 or NaH_2PO_4 (0.2 M) was added to maintain the pH at 7.2. All the serum bottles were incubated at 37°C in a constant temperature gas bath oscillator at a rate of 210 rap min^{-1}, protected from light.

Table 1
Sources of chemicals

Serial number	Reagent	Specification	Manufacturer
1	Diammonium phosphate ($(NH_4)_2HPO_4$)	Analytically pure (AR)	Sinopharm Chemical Reagent Co., Ltd.
2	Orange G (OG)	AR	Sinopharm Chemical Reagent Co., Ltd.
3	hydrochloric acid (HCl)	AR	Sinopharm Chemical Reagent Co., Ltd.
4	Sodium chloride (NaCl)	AR	Sinopharm Chemical Reagent Co., Ltd.
5	Sodium hydroxide (NaOH)	AR	Sinopharm Chemical Reagent Co., Ltd.
6	Potassium bromide (KBr)	AR	Sinopharm Chemical Reagent Co., Ltd.
7	$Na_2S·9H_2O$	AR	Sinopharm Chemical Reagent Co., Ltd.
8	Na_2CO_3	AR	Sinopharm Chemical Reagent Co., Ltd.
9	$NaHCO_3$	AR	Sinopharm Chemical Reagent Co., Ltd.
10	Na_2HPO_4	AR	Wuxi Jingke Chemical Co., Ltd.
11	NaH_2PO_4	AR	Wuxi Jingke Chemical Co., Ltd.
12	NaCl	AR	Shanghai Alliance Chemical Reagent Co., Ltd.
13	NaOH	AR	Shanghai Alliance Chemical Reagent Co., Ltd.
14	H_2SO_4	AR	Shanghai Alliance Chemical Reagent Co., Ltd.
15	Na_2SO_4	AR	Shanghai Alliance Chemical Reagent Co., Ltd.
16	CH_2Cl_2	Chromatographic purity	Shanghai Alliance Chemical Reagent Co., Ltd.
17	Na_2S	AR	Sinopharm Chemical Reagent Co., Ltd.

2.5. Biological decolorization of OG

A series of batch experiments were conducted to determine whether RSB could promote the biological decolorization of an azo dye. A flask experiment was conducted in 100 mL serum bottles, sealed with a butyl rubber stopper, containing buffered medium at a pH of 7.2 with Na_2HPO_4 and NaH_2PO_4 (0.2 M). When investigating the effect of pH, Na_2HPO_4, and NaH_2PO_4 (0.2 M) were used to control the pH at 6–8, while Na_2CO_3 and $NaHCO_3$ (0.1 M) were added to control the pH at above 8. Basal nutrients are shown in Table 2.

OG (5 mL, 1 g L^{-1}) and 95 mL basal nutrient medium were added to a serum bottle. Buffer was added to maintain a neutral situation. Domestic AGS and RSB were added to the serum bottle. The bottles were sealed with butyl rubber stoppers, and the gas headspace was flushed for two min with oxygen-free flushing gas (N_2). Finally, the prepared serum bottle was shocked in a thermostatic gas bath shaker at 37°C and 180 rap min^{-1} without light. At selected time intervals, 4 mL reaction solution was sampled with a 5 mL syringe. After filtration through a 0.45 μm microporous membrane, the sample was placed in a 5 mL centrifuge tube for subsequent measurement.

The concentration of AGS, RSB dosage, pH, carbon source, and carbon source dosage were varied to study their effects on the reductive decolorization of azo dye OG, the total organic carbon (TOC) decolorization of OG, and decolorization products (by gas-chromatography and mass spectrometry (GC-MS)), and to postulate a decolorization pathway for the RSB/AGS system with OG.

To investigate the long-term biological decolorization of OG, laboratory-scale UASB reactors (effective volume 4 L) were established and initiated with 15 g L^{-1} AGS and a basal nutrient medium (2,000 mg of COD L^{-1}). Fig. 1 illustrate

Table 2
Nutrient solution formula

Macroelement	
Reagent	Dosage (mg L^{-1})
NH_4Cl	280
KH_2PO_4	250
$MgSO_4·7H_2O$	100
Glucose	1,000
Sodium formate	500
Sodium acetate	500
Sodium propionate	500
$CaCl_2$	5.7
$FeCl_2·4H_2O$	2.0
$CoCl_2·6H_2O$	1.0
$NiCl_2·6H_2O$	1.0
$MnCl_2·4H_2O$	0.5
Boric acid (H_3BO_3)	0.05
$ZnCl_2$	0.05

a running UASB reactor unit, showing inlet water being peristaltically pumped to the top of the reactor using the inlet mode of downflow, which creates an upflow effect at the bottom of the reactor. The HRTs of the reactors were kept constant within the range 5–5.5 h. When the COD removal rate of the effluent reached 80%, OG was added to the reactor, with the concentration of dye increasing from 50 to 150 mg L^{-1}. The day on which dye was first added to the reactor influents was defined as day 0 of the reactor operation. After a 60 d start-up phase in the absence of RM, RSB was added to the influent at a dosage of 1.2 g, 500 mL
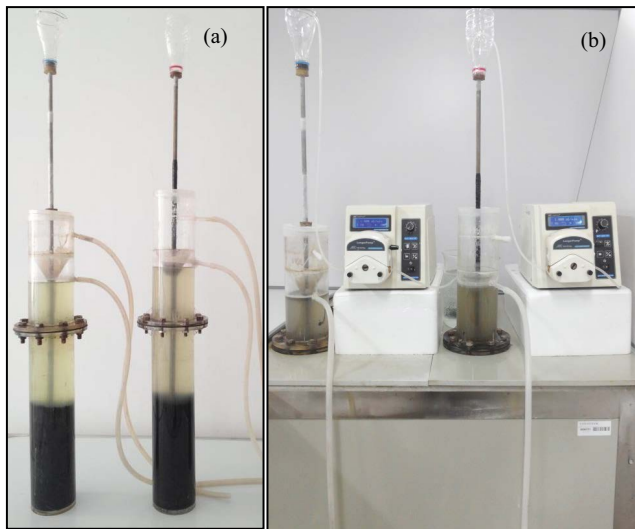
Fig. 1. (a) Physical picture of UASB reactor and (b) working diagram of UASB reactor.

effluent was collected every day and retained for subsequent measurement. The effect of effluent from the UASB reactor before and after the addition of RSB was observed. The azo dye decolorization pathway was investigated by TOC analysis and GC-MS.

2.6. Analytical methods

The concentration of OG was monitored by measuring the maximum absorbance at λ = 479 nm with a UV-vis spectrophotometer (1600PC, Mapada Co., Shanghai) equipped with quartz cuvettes of 1 cm light path. The wavelength scan (200–650 nm) of OG during decolorization was also performed on this spectrophotometer. Before testing, the samples were filtered through 0.45 μm membrane. The total mineralization of OG was measured by using the removal of TOC by a TOC-LCPH analyzer (Shimadzu Co., Japan). The decolorization products were determined by GC-MS (Agilent 7800A/597, USA) with a 5C HP-5 capillary column (20 m × 320 μm × 0.25 μm). The pretreatment process and test method were as followed. Prior to extraction, the samples were filtered through 0.22 μm filter membrane. The pH of the obtained samples was acidified to 2 with H_2SO_4. An appropriate amount of NaCl was then added. The extraction procedure was repeated with dichloromethane for three times to ensure that the products were completely transferred into the dichloromethane, and then the samples were dehydrated with Na_2SO_4. The extract was finally concentrated to 1–2 mL with a rotary evaporator at 40°C for further testing. The decolorization products were determined by GC-MS with a with HP-5 capillary column. The sample was injected using splitless injection mode. The GC parameters used were an injector temperature of 250°C with an injection volume of 1 μL; helium as carrier gas at a flowrate of 1.0 mL min⁻¹. The oven temperature programmed from 40°C (keeping for 2 min) to 100°C at 12°C min⁻¹, then increased at 5°C min⁻¹ to 200°C, and lastly increased at 20°C min⁻¹ to 270°C remaining constant for 2 min. For quantification, the mass spectrometric detector (MSD) was operated in an electron impact ionization mode with an ionizing energy of 70 eV, with the ion source temperature at 300°C. Nist-11 standard library was used to identify the degradation products, and the matching degree was more than 90%.

3. Results and discussion

3.1. Characterization of RSB

The textural characterization of RSB by BET is shown in Table 3. These samples all have a certain amount of specific surface area, which increases with the concentration of $(NH_4)_2HPO_4$. The specific surface area of RSB_0 is probably since straw itself contains oxygen and in the process of carbonization, the oxidation reaction of straw results in the etching of carbon. The biochars being immersed in $(NH_4)_2HPO_4$ have a much higher specific surface area than the directly carbonized. This phenomenon is consistent with the report of Benaddi et al. [22], indicating that $(NH_4)_2HPO_4$ is a suitable activator.

SEM was conducted to examine the porous nature of RSB, result shows that the samples immersed in $(NH_4)_2HPO_4$ have more micropores, whose diameters are smaller than RSB_0 (Fig. 2). This result is consistent with BET, indicating that being immersed in $(NH_4)_2HPO_4$ can promote the development of pores and enhance the thermal stability of straw.

FT-IR analysis was performed to determine the functional groups in RSB. As shown in Fig. 3, different kinds of RSB have similar peaks. Peaks at 3,450 cm⁻¹ could be caused by the stretching vibration of –OH, while those at 2,928; 1,650; 1,398; and 1,088 cm⁻¹ could be ascribed to the symmetric and asymmetric stretching vibrations of –CH₃ and –CH₂, the stretching vibration of –C = O, and the symmetric and asymmetric stretching vibrations of –COOH and C–O [23–25]. Furthermore, after RSB was immersed in $(NH_4)_2HPO_4$, a new peak appeared at 750 cm⁻¹, which may be assigned to the bending vibration of –COH [26].

Raman spectroscopy has proven to be a powerful local structural probe. All the spectra exhibited typical Raman characteristics of RSB with a G-band appearing in the region of 1,590–1,610 cm⁻¹ and a D-band appearing at 1,350–1,380 cm⁻¹ (Fig. 4). The G-band corresponds to Raman-active E_2g, which is due to vibration mode corresponding to the movement in opposite directions of two neighboring carbon atoms and the D-band is associated with the presence of defect [27]. For our samples, I_D are all lower than I_G, indicating that the immersing and heating process significantly reduces structural disorder in RSB. The pH_{pzc} of RSB was determined to be 6.62.

Table 3
Textural parameters of RSB

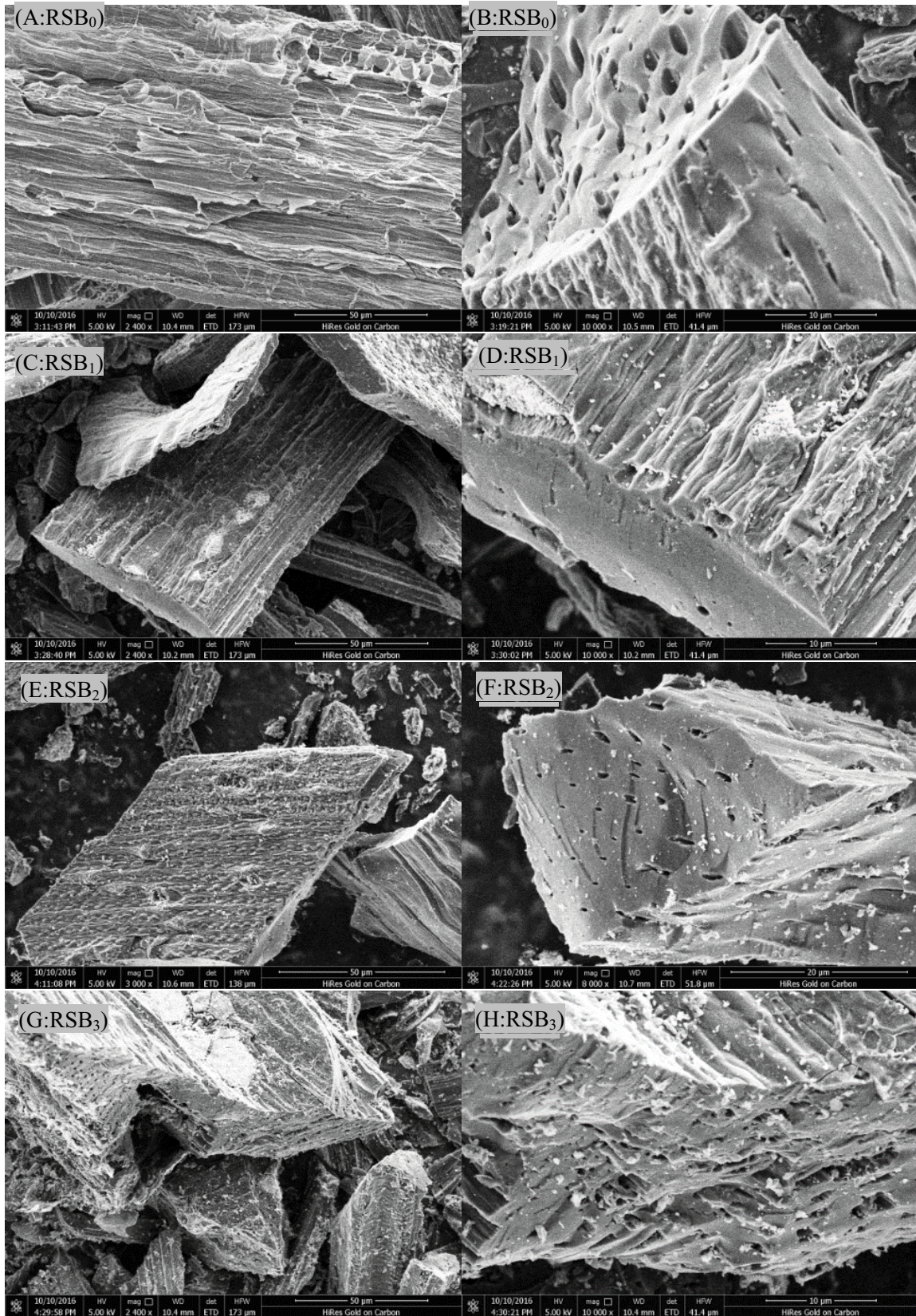| Samples	S_{BET} (m² g⁻¹)	V_{total} (cm³ g⁻¹)	V_{mic} (cm³ g⁻¹)	d_p (nm)
SAC_0	31.4	0.0267	0.0038	3.3973
SAC_1	231.1	0.1249	0.0878	2.1620
SAC_2	265.4	0.1501	0.0783	2.2623
SAC_3	287.8	0.1576	0.1005	2.1896

Fig. 2. SEM images of RSB. (a and b) RSB_0, (c and d) RSB_1, (e and f) RSB_2, and (g and h) RSB_3.

3.2. Chemical decolorization of OG

Decolorization effects of OG in different systems are shown in Fig. 5. In Na_2S/RSB_3 system, the decolorization rate of OG can reach 100% in 90 min, which is greatly higher than that in the systems of Na_2S or RSB_3 alone and even their sum.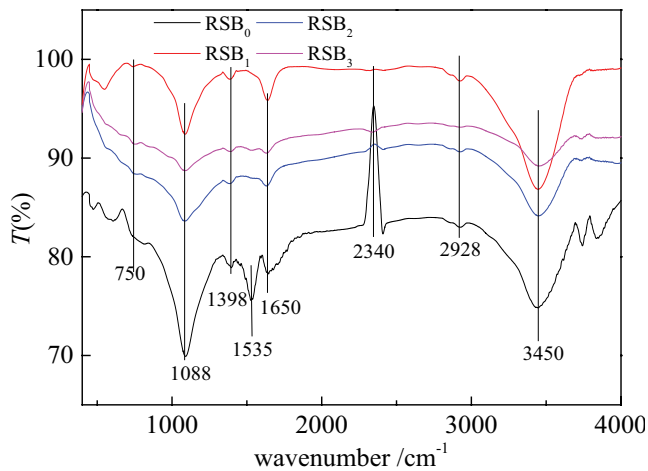 There was very limited reduction in the presence of Na_2S alone or RSB_3 alone, which proves the function of RSB_3 as a RM in the chemical decolorization of OG. Similar results have been found in Pereira et al. [28].

To determine the effect of RSB on OG decolorization, different RSBs were tested in OG decolorization in the absence and presence of Na_2S, with 0.3 g L^{-1} RSB dosage, 10 mM Na_2S, and pH 7.2. After 150 min, the adsorption of OG by RSBs alone were 6.1%, 4.7%, 11.1%, and 21.5% for RSB_0, RSB_1, RSB_2, and RSB_3, respectively; while the decolorization rates of OG increased to 99.3%, 81.7%, 93.6%, and 100% after the addition of Na_2S (Fig. 6). It can be concluded that RSB_3 has the best adsorption effect on OG, as well as its ability to enhance Na_2S reducing and decolorizing OG. The apparent rate constant of OG was the largest in the RSB_3/Na_2S system, demonstrating that RSB_3 was most favorable for enhancing OG decolorization. This result might be attributed to the larger specific surface area of RSB_3 (Table 3), which increases the probability of contact between OG and RSB_3 [29], and thus facilitating electron transfer from Na_2S to OG for decolorization. At the same time, the infrared spectrum of RSB_3 shows that a new oxygen-containing functional group with C=N bond is added to its structure, which may also be the reason for accelerating the reduction and decolorization of OG by Na_2S [30,31]. RSB_3 was used in the following experiments.

The effect of the RSB_3 dosage is presented in Fig. 7. The OG decolorization was enhanced as the RSB_3 dosage
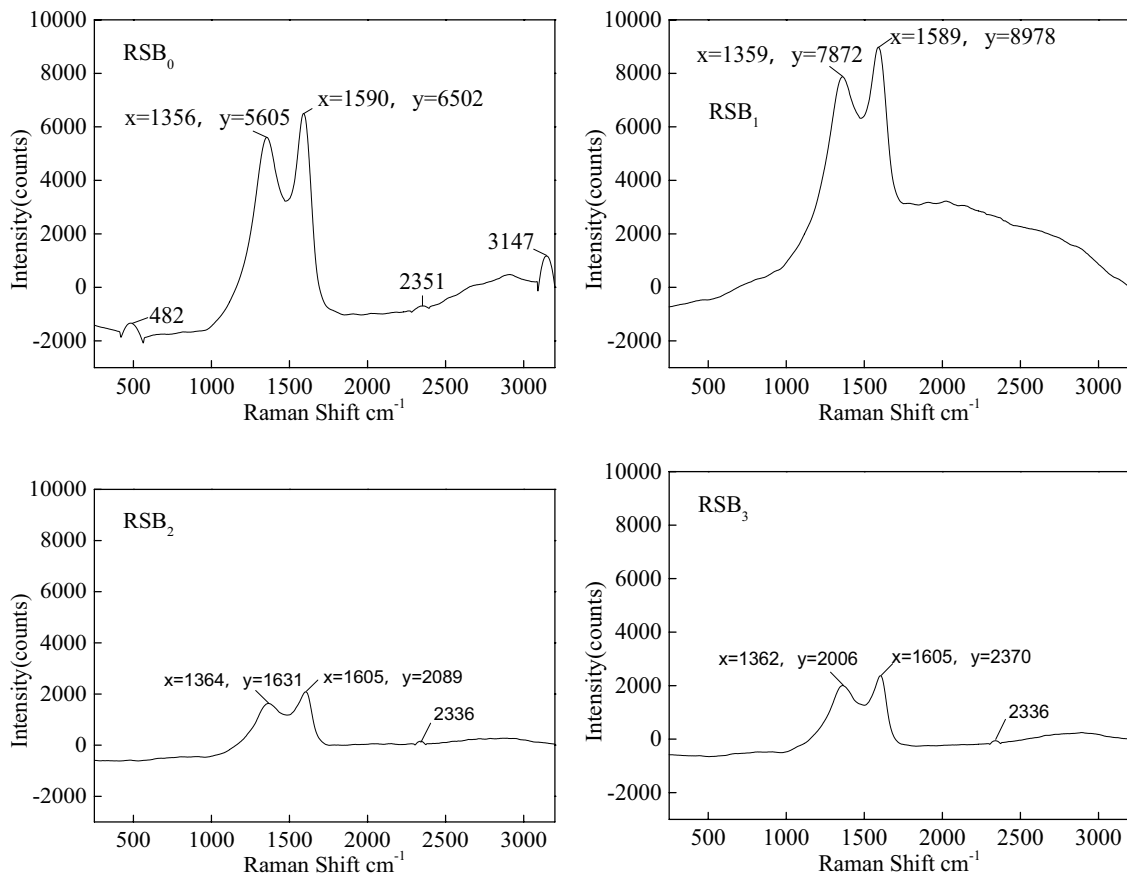
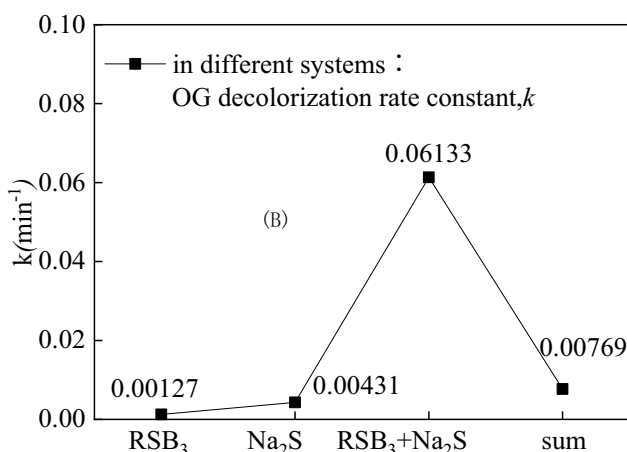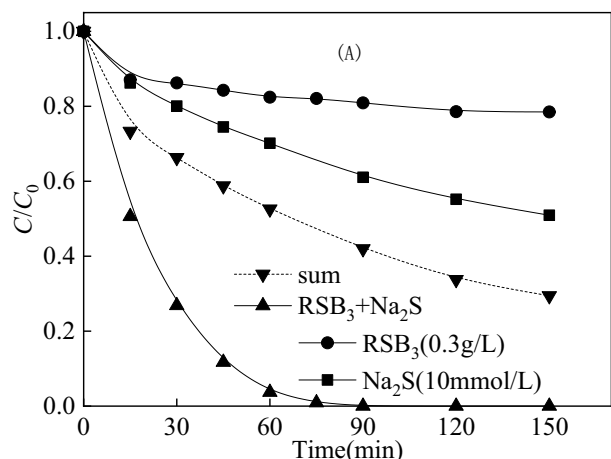Fig. 3. FT-IR spectra of RSB.

Fig. 4. Raman spectra of RSB.

Fig. 5. (a) Decolorization of OG in different systems and (b) OG decolorization rate constant in different systems. Experimental conditions: $[OG]_0$ = 20 mg L^{-1}, $[RSB]_0$ = 0.3 g L^{-1}, $[Na_2S]_0$ = 10 mM, pH 7.2, and 37°C.

Fig. 6. Effect of different RSB on the decolorization of OG in the absence and presence of Na_2S. Experimental conditions: $[RSB]_0$ = 0.3 g L^{-1}, $[Na_2S]_0$ = 10 mM, and pH = 7.2.

Fig. 7. (a) Effect of RSB_3 dosage on the degradation of OG by Na_2S and (b) OG decolorization rate constant with different dosage of RSB_3. Experimental conditions: [OG] = 20 mg L^{-1}, $[Na_2S]$ = 10 mM, and pH = 7.2.

increased. At an RSB_3 dosage ranging from 0.1 to 0.3 g L^{-1}, the decolorization rate of OG increased from 71.4% to 100% (Fig. 7a). When the RSB_3 dosage increased to 0.5 g L^{-1}, the OG was completely decolorized after 45 min, and the apparent rate constants (k) of OG decolorization were 0.00827, 0.01596, 0.06133, 0.08634, and 0.12267 min^{-1} for increasing dosages of RSB_3 (0.1, 0.2, 0.3, 0.4, and 0.5 g L^{-1}, respectively) (Fig. 7b). On the one hand, the slow rate of reduction of OG by Na_2S alone indicates that the electron transfer rate between Na_2S and OG is not high; at the same time, in the RSB_3/Na_2S system, the reaction rate is significantly increased, which proves that RSB_3 can accelerate the electron transfer. Similar results also appeared when Fu and Zhu [32] studied that graphite oxide (GO) promoted the reduction of nitrobenzene by Na_2S. It was found that when the dosage of GO was 5 mg L^{-1}, the reaction rate was 100 times of that without GO. On the other hand, when the OG concentration was constant, increasing the dosage of RSB_3 could increase the specific surface area and active site of adsorption, so that the decolorization rate of OG significantly stimulated by increasing RSB dosage.

The effect of Na_2S concentration on the decolorization of OG was evaluated in the RSB_3/Na_2S system. As the Na_2S
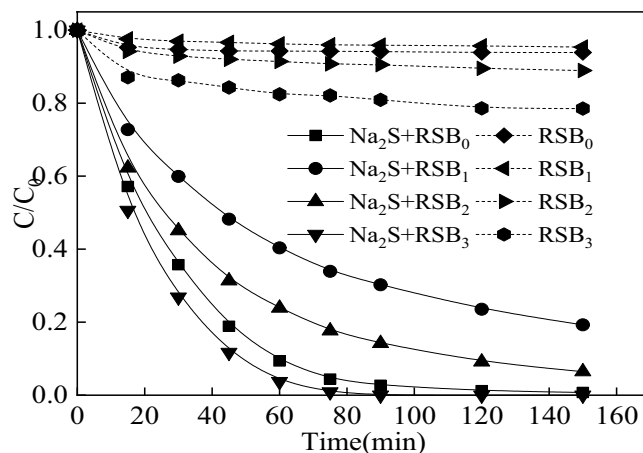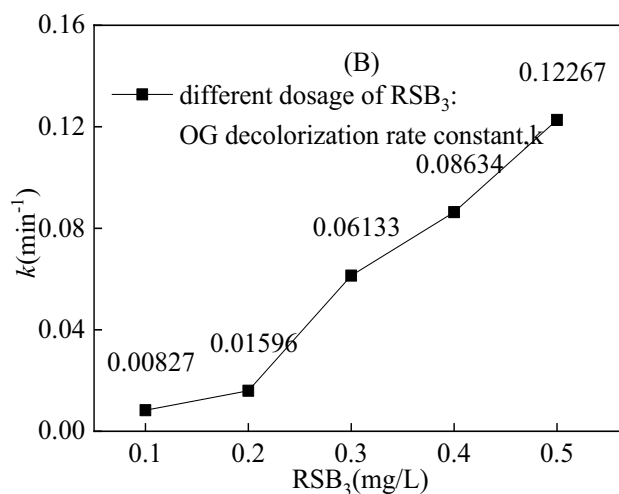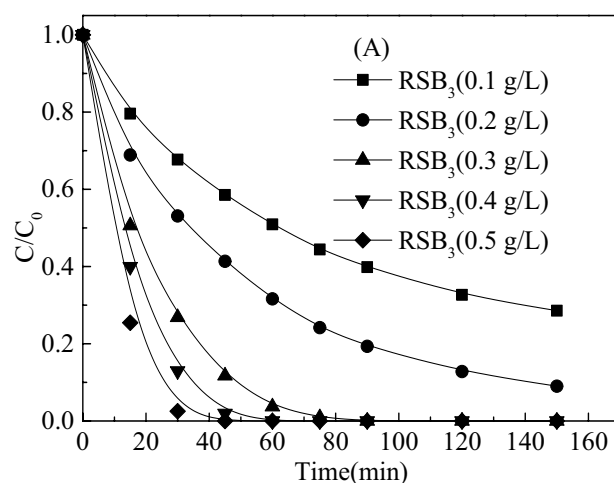
concentration increased from 2 to 10 mM, the time required for complete decolorization of OG was reduced from 150 to 90 min. However, when the concentration of Na_2S was further increased to 20 mM, the time for the complete decolorization did not decrease significantly (Fig. 8a). At increasing concentrations of Na_2S, the apparent rate constant of OG was 0.03369, 0.04593, 0.06133, 0.06550, and 0.08326 min^{-1} with 2, 5, 10, 15, and 20 mM Na_2S, respectively (Fig. 8b). Na_2S in the RSB_3/Na_2S system acts as an electron donor, hence the higher the Na_2S concentration, more electrons are supplied to decolorize OG [33,34].

We further evaluated pH effect on OG decolorization. As shown in Fig. 9, OG was completely decolorized after 60 min at pH 6.0, but the decolorization decreased as the pH increased. This phenomenon may be related to the pH_{pzc} of RSB_3 [35]. The same as activated carbons, RSB is a material with amphoteric character; thus, depending on the pH of the solution, their surfaces might be positively or negatively charged [36]. At pH > pH_{pzc} (6.62), the surface of RSB_3 is negative, which is unfavorable for the adsorption of anionic OG. Moreover, the electrostatic repulsive force between RSB_3 and OG is not conducive to electron transfer between RSB_3 and OG at a high pH, so the decolorization efficiency of OG is lower than that at lower pHs.
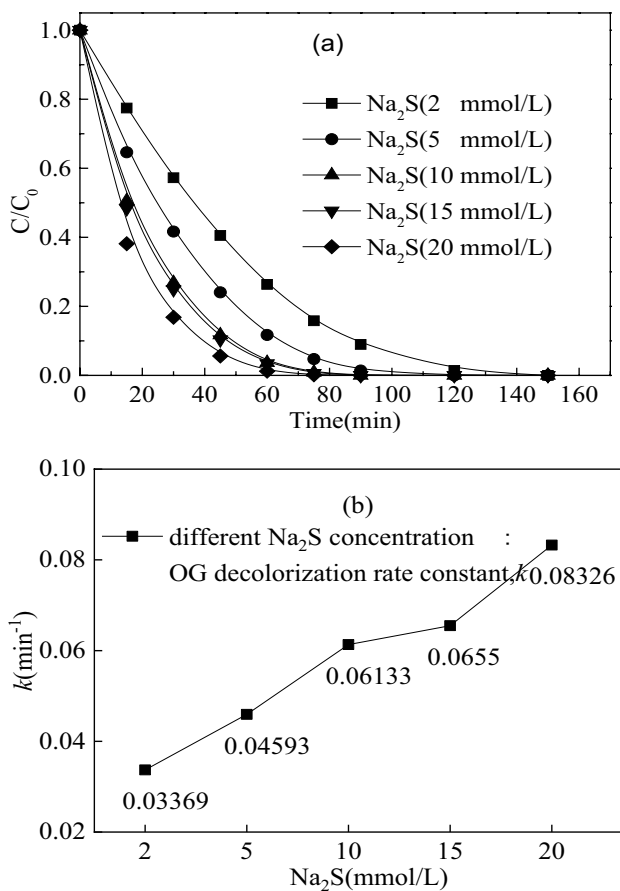
Due to the large variation in temperature in actual dye wastewater, it is necessary to study the effect of temperature on OG decolorization in the RSB_3/Na_2S system. When the temperature was 20°C, the decolorization rate of OG was 92.8% after 150 min, while when the temperature was raised to 60°C, OG was completely decolorized after 60 min (Fig. 10a). This result suggested that higher temperature is favorable for the decolorization of OG. Increasing the temperature increases the transfer rate of electrons in the reaction system, making the OG molecules more accessible to the electrons to allow reductive decolorization [37]. The Arrhenius formula was fitted to the apparent rate constants of OG decolorization at different temperatures, and the activation energy (Ea) was determined to be 39.96 kJ mol^{-1} (Fig. 10b).

3.3. Biological decolorization of OG

In the absence of RSB, the decolorization rate of OG by AGS alone was only 53.7% over 48 h (Fig. 11a), with the apparent decolorization rate constant being 0.01567 min^{-1} (Fig. 11b). After addition of RSB, the decolorization of OG increased to 83.5% in the AGS/RSB_3 system, higher than the sum of OG decolorization in the presence AGS or RSB alone. As RM, RSB can shuttle the electrons from organic carbon substrate to AGS to enhance the decolorization of azo bonds.

Evidence indicates that biological activity played an important role in the decolorization of OG. As the AGS dosages increase from 10 to 30 g L^{-1}, the decolorization rate increases from 52.7% to 72.2% within 48 h. With a further increase in the AGS dosage to 50 g L^{-1}, however, only a slight enhancement was observed (Fig. 12). This proves that the AGS contained specialized bacteria transferring reducing equivalents to OG while metabolizing the substrates [4]. An increased AGS dosage leads to a rise in the rate of carbon consumption and the release of more electrons, which fully utilizes the ability of RSB_3 to transfer electrons, thereby increasing the decolorization rates of OG. However, the action of RSB_3 has an upper limit; once the AGS concentration becomes too high, excess electrons cannot be transferred
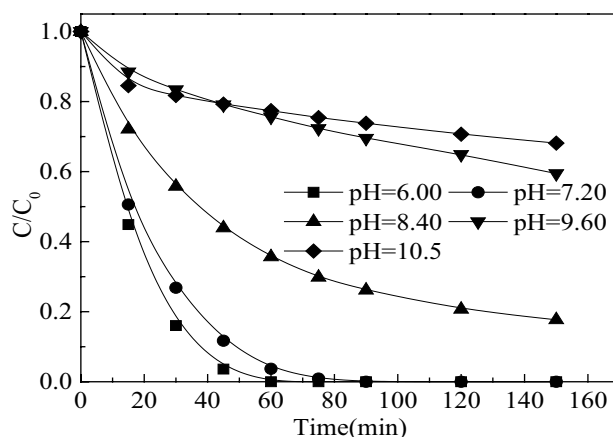
Fig. 8. (a) Effect of Na_2S concentration on the degradation of OG and (b) OG decolorization rate constant with different concentrations of Na_2S. Experimental conditions: $[OG]_0$ = 20mg L^{-1}, $[RSB_3]_0$ = 0.3g L^{-1}, and pH = 7.2.

Fig. 9. Effect of initial pH on the decolorization of OG $[RSB]_0$ = 0.3 g L^{-1}, $[Na_2S]_0$ = 10 mM, and 37°C.

to OG via RSB_3 in time, so that the OG decolorization rate begins to decrease. Similar behavior was observed for the dosage of RSB_3. When the RSB_3 dosage increased from 0.1 to 0.4 g L^{-1}, the decolorization rate of OG increased from 61.0% to 84.6% after 48 h, while when the dosage of RSB_3

increased to 0.5 g L^{-1}, the OG decolorization rate increased only slightly. The larger the dosage is, the stronger the ability to transfer electrons is, and the more easily electrons transfer to OG, which significantly increases the decolorization rate of OG.

The primary electron donor in biological dye decolorization may play an important role in OG decolorization [38]. Therefore, the substrate type and concentration may affect the OG decolorization rate. Glucose, sodium formate, sodium acetate, sodium propionate, and a mixture of them were used as carbon sources to compare the effects of different substrates on OG decolorization. Fig. 13 represents the dye decolorization rate as a function of the reaction time. Better decolorization was achieved in the order: mixed carbon source > sodium propionate > glucose > sodium formate > sodium acetate > no carbon source. Furthermore, when sodium propionate is used as the carbon source, the decolorization rate of OG is 72.1%, which is closest to the value of 72.2% for the mixed carbon source. Therefore, sodium propionate is taken as an example to investigate the effect of the carbon source dosage on dye decolorization. The decolorization rate increased sharply with the
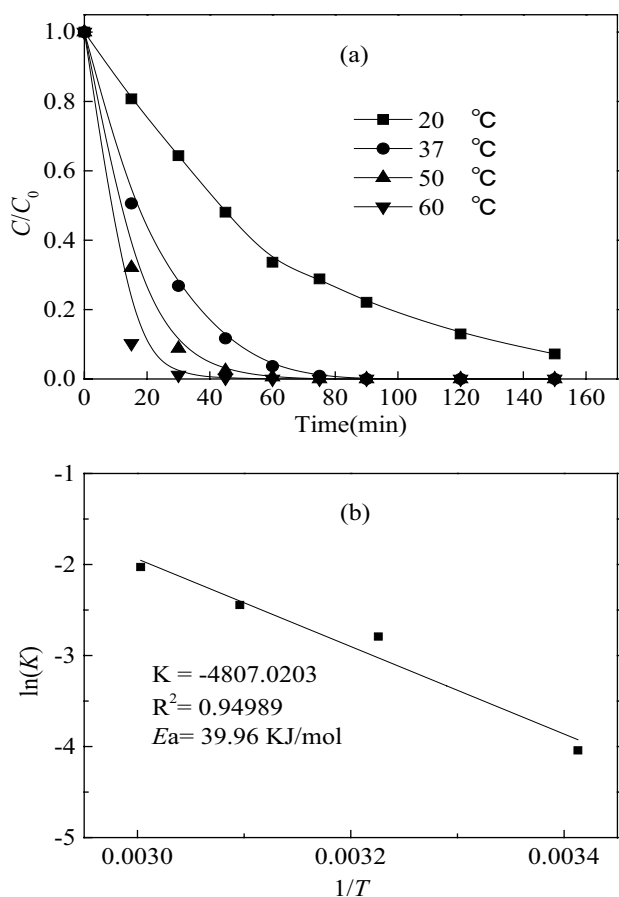

Fig. 10. (a) Effect of temperature on RSB_3 to promote Na_2S for OG degradation and (b) the Arrhenius plot of ln$k$ vs. $1/T$ of the decolorization of OG. Experimental conditions: $[OG]_0 = 20$ mg L^{-1}, $[RSB_3]_0 = 0.3$ g L^{-1}, and pH = 7.2.
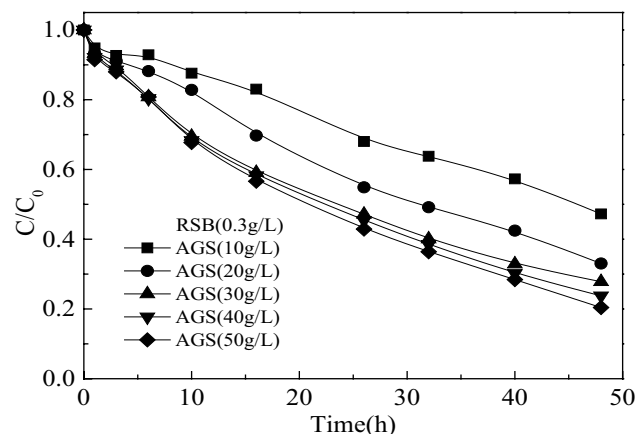

Fig. 12. Effect of AGS dosage on the decolorization of OG $[OG]_0 = 50$ mg L^{-1}, $[RSB]_0 = 0.3$ g L^{-1}, pH 7.2, and 37°C.
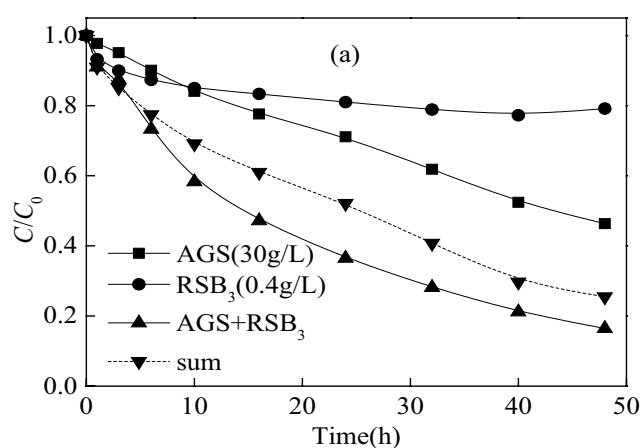
Fig. 11. (a and b) Decolorization of OG in different systems $[OG]_0 = 20$ mg L^{-1}, $[RSB]_0 = 0.3$ g L^{-1}, $[AGS]_0 = 10$ mM, pH 7.2, and 37°C.
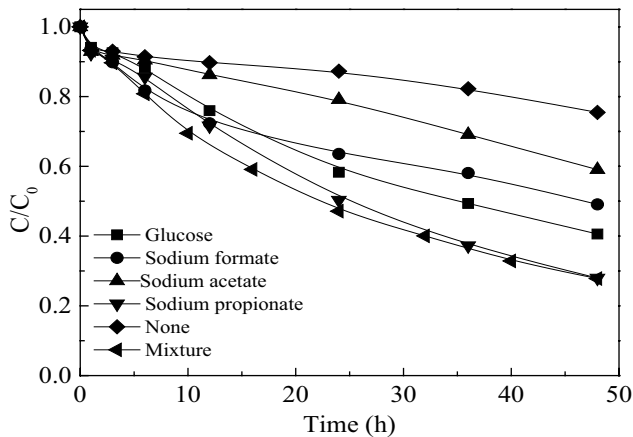
Fig. 13. Effect different carbon source types on the decolorization of OG $[OG]_0$ = 20 mg L^{-1}, $[RSB]_0$ = 0.3 g L^{-1}, $[AGS]_0$ = 30 mM, pH 7.2, and 37°C.

Fig. 14. Effect of carbon sources dosage on OG decolorization $[OG]_0$ = 20 mg L^{-1}, $[RSB]_0$ = 0.3 g L^{-1}, $[AGS]_0$ = 30 mM, pH 7.2, and 37°C.

sodium propionate dosage up to 2.5 g L^{-1}. However, when the sodium propionate dosage was increased to 3.5 g L^{-1}, the OG decolorization rate was 87.3%, which did not represent a significant increase (Fig. 14). The addition of a carbon source is a prerequisite for the AGS reduction and decolorization of OG. AGS generates extracellular reductase or transfers electrons by consuming an additional carbon source to degrade and decolorize OG. The higher the concentration of sodium propionate is the more electrons are released after being absorbed by AGS, which results in more electrons being transferred to OG through RSB_3, and a higher rate of OG decolorization. However, if the amount of sodium propionate continues to increase, the upper limit of the electron transfer amount of RSB_3 will be reached for its microporous structure and limited surface groups, so that excess sodium propionate will be wasted, thus the decolorization rate of OG will not continue to increase.

The effect of RSB on the decolorization of azo dyes was also studied in a continuous flow UASB reactors. The reactor was initiated with 1.5 g L^{-1} AGS and fed with nutrient medium. OG (50–150 mg L^{-1}) was added to the influent after a 45 d start-up stage, during which time, the COD in the effluent was less than 200 mg L^{-1} (Fig. 15), then the reactor operation was continued. The moment of dye addition was defined as the start of the experiment (0 d in Fig. 16). The concentration of OG in the effluent increased continuously with that in the influent up to 60 d, reaching 46 mg L^{-1}. After RSB_3 was added for 40 d, the dye removal efficiency increased considerably from 69% to 83%. The results from this continuous experiment implied that RSB played an important role in improving the decolorization of azo dye.

3.4. Mechanism

3.4.1. Product analysis

Fig. 17 shows the UV-Vis spectra of OG during its decolorization in the RSB_3/Na_2S system. OG has the absorption peak at 479 and 330 nm, characteristics of azo bond and naphthalene nucleus, respectively [33]. As the reaction
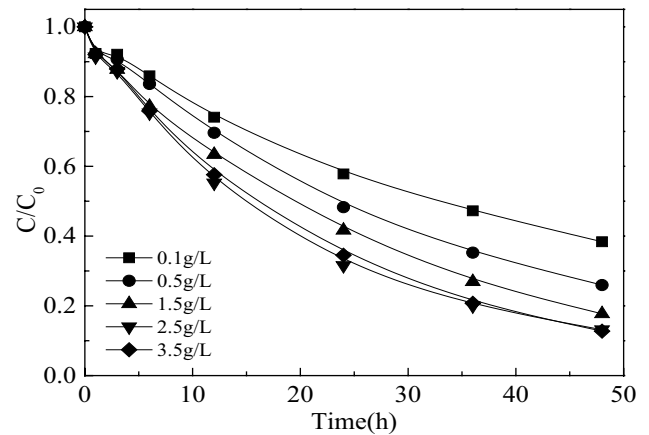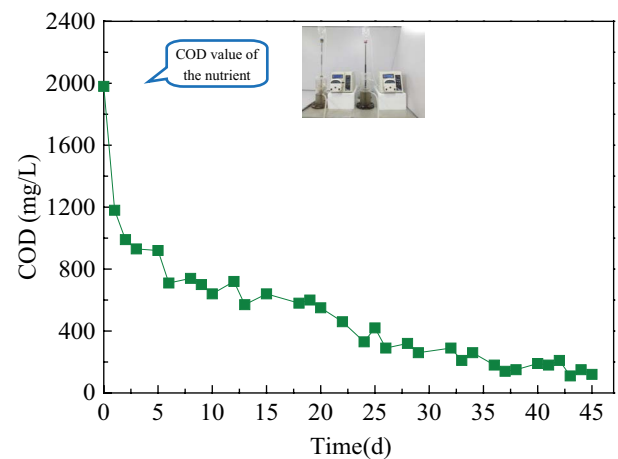

Fig. 15. COD value changed of continuous flow UASB reactor.

proceeds, the peak intensities of OG at 479 and 330 nm are decreased, indicating that the azo bond and naphthalene nuclei of OG molecules cleaved. The above peaks completely disappeared after 150 min. OG molecules receive electrons continuously to be reduced, leading to disruption of azo bonds and naphthalene nuclei, so that the azo dye is decolorized.

GC/MS was used to identify the intermediate products of OG decolorization. As shown in Table 4, in both the RSB_3/AGS and RSB_3/Na_2S systems, the intermediates mainly consist of N-containing compounds and aromatic amines, while O-containing aromatic compounds are fewer, confirming that in the process whereby RSB_3 promotes the reduction and decolorization of OG by Na_2S, the electron transfer finally acts on the chromophore of the azo bond, while damage to the benzene ring is limited. In addition, more products arise from the RSB_3/AGS system, which indicates that OG underwent deeper decolorization in the anaerobic biological system.
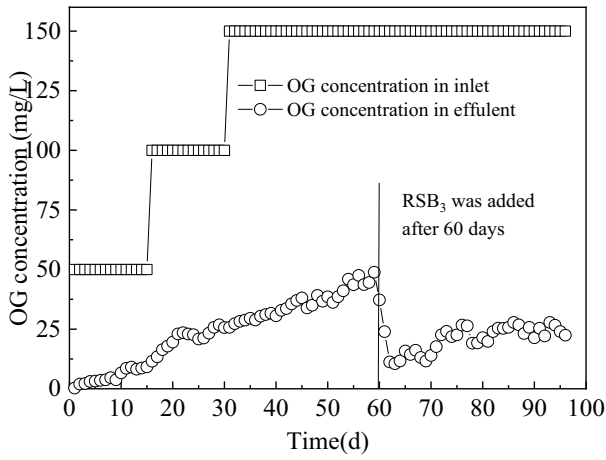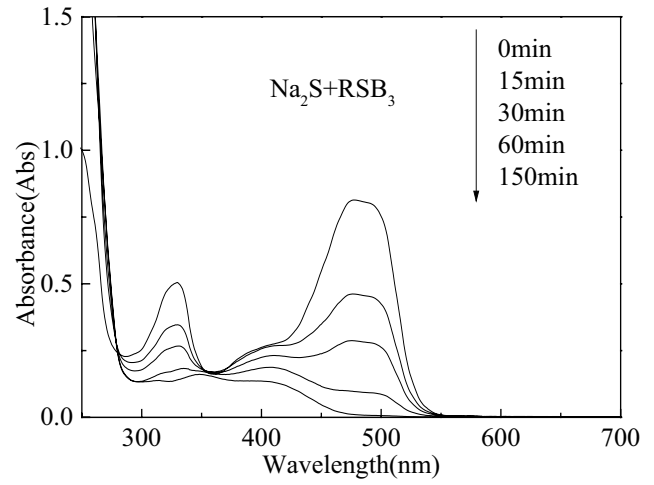
Fig. 16. OG degradation rate changes in the effluent of UASB reactor.

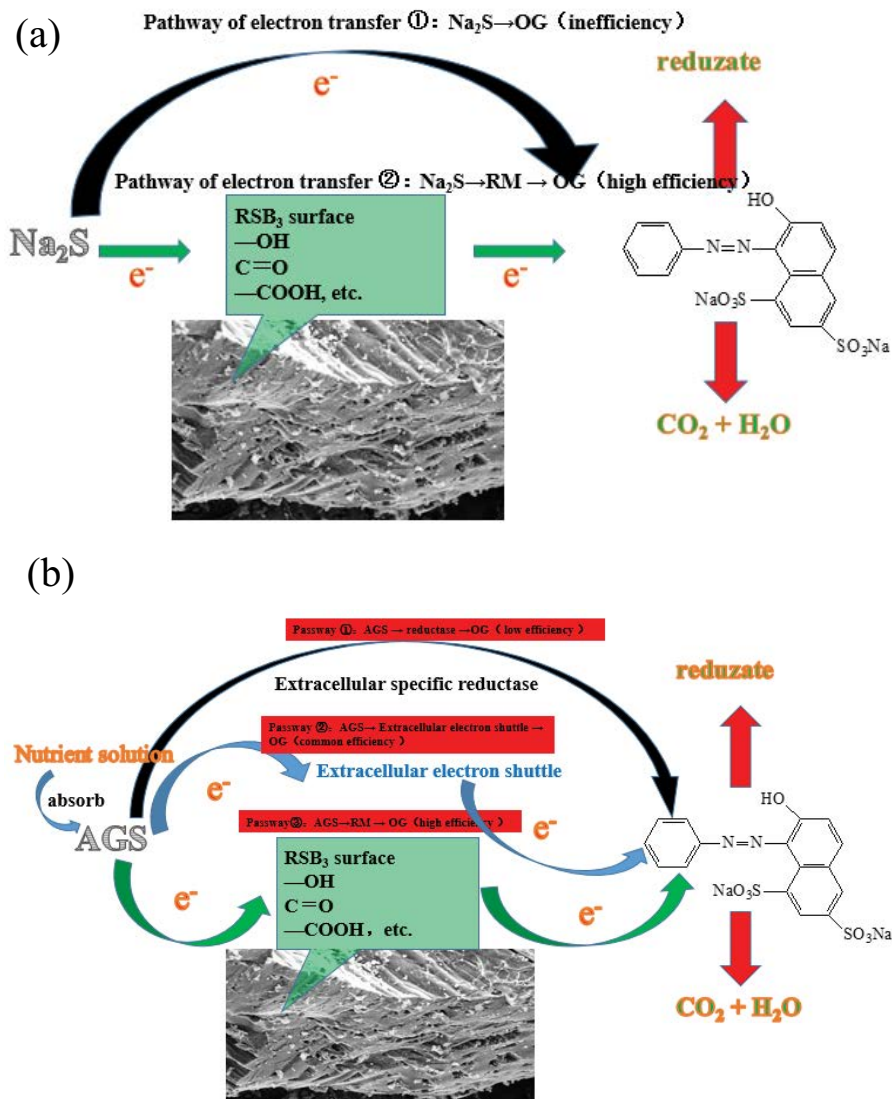Fig. 17. UV-Vis spectra and TOC changes for OG decolorization.

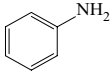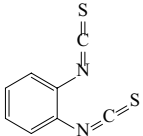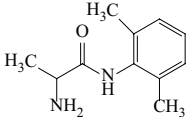Fig. 18. Schematic diagram of OG degradation (a) Na_2S in presence of RSB_3 and (b) AGS in presence of RSB_3.

Table 4
Intermediate products of OG decolorization

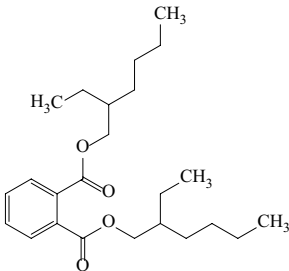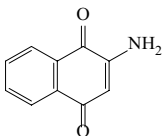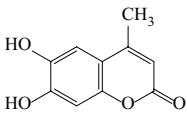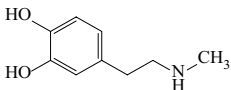| Compound	Constitutional formula	Molecular formula	RSB$_3$/AGS	RSB$_3$/Na$_2$S
Aniline		C_6H_7N	Y	Y
1,2-Phenylene diisothiocyanate		$C_8H_4N_2S_2$	–	Y
N-(2-Aminopropionyl)-2,6-xylidine		$C_{11}H_{16}N_2O$	Y	Y
Sulfur powder, precipitated		S_8	–	Y
Bis (2-Ethylhexyl) phthalate		$C_{24}H_{38}O_4$	–	Y
2-amino-1,4-naphtha quinone		$C_{10}H_7NO_2$	Y	–
4-methylesculetin		$C_{10}H_8O_4$	Y	–
N-2-(3,4-dihydroxyphenyl) ethylmethylamine		$C_9H_{13}NO_2$	Y	–

Y means the products were detected.

3.4.2. Chemical decolorization of OG

From the characterization results of RSB$_3$ (Fig. 18a), we can observe the pore structure and many surface functional groups that play an important role in electron transfer between OG and Na$_2$S, greatly improving the rate of electron transfer and indirectly increasing the rate of OG decolorization.

Fig. 19 shows an analysis of the pathway of OG reduction and decolorization in the RSB$_3$/Na$_2$S system. In the experiment, the solution containing OG gradually lightened from orange to colorless, which indicated that the chromogenic azo bond of OG was broken, and the result of UV-Vis scanning during the reaction also confirmed this point. The OG decolorization pathway is as follows. OG as electron acceptor is reduced after receiving electrons, and the molecular structure of –N=N– transforms to –NH–NH–, and then continues to transform to R$_1$–NH$_2$ and R$_2$–NH$_2$, further degrading to small molecule acids and eventually mineralizing to H$_2$O and CO$_2$ [7].
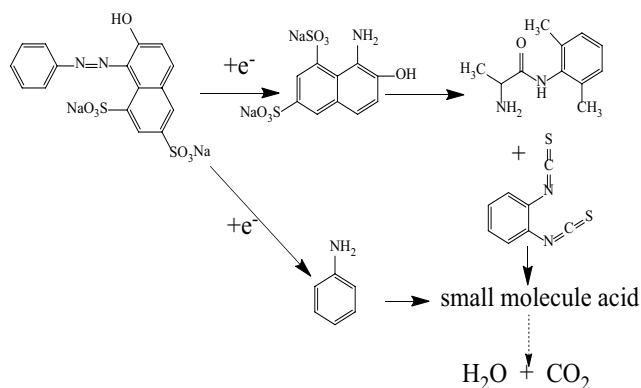
Fig. 19. Degradation pathway of Azo dye OG.

3.4.3. Biological decolorization of OG

The addition of RSB_3 to the AGS system can accelerate the rate of OG decolorization. The principle of OG decolorization is shown in Fig. 18b. There are three ways to degrade OG. (1) The reduction equivalent produced by the oxidizing substrate is transferred to OG by nonspecific enzymes produced by microorganisms in AGS. (2) There are specific azoreductases under anaerobic conditions in the environment or in sewage treatment systems. Specific azoreductases under anaerobic conditions in sewage treatment systems stimulate the transformation of electrons to OG, causing its reduction and decolorization. (3) Microorganisms in AGS channel from the oxidized nutrient solution to electron-accepting groups on RSB. The reduced RSB then transfer the electrons to reduce OG [39–41]. In pathway one, the low permeability of the cell membranes for the highly polar sulfonated azo compounds leads to the limited ability of enzymes to reduce azo dye [42]. In pathway two, the amount and performance of extracellular electron shuttling determines the rate of electron transfer, while in the environment, extracellular electron shuttles are usually rare, so their performance is poor. In pathway three, the addition of RM is controllable. Certain amount of RM can improve electron transfer significantly, so it is more suitable for practical engineering applications. In the RSB_3/AGS system, RSB_3 as an additional RM contains pores and abundant surface functional groups in its structure. The electron transfer efficiency of RSB_3 plays an important role in electron transfer between AGS and OG, greatly improving it. An increase in the rate of electron transfer indirectly increases the rate of OG reductive decolorization.

4. Conclusion

The biochar was synthesized from rice straw by chemical/thermal treatment, and then characterized by FTIR, BET, SEM, and Raman spectra. RSB possessed oxygen-functional groups on the surface, which could act as redox mediators in the decolorization of azo dye. Indeed, RSB could significantly accelerate the chemical reduction of OG with Na_2S as the electron donor. Moreover, addition of RSB could enhance the decolorization rate of OG in the anaerobic biological process, since the oxygen group on RSB could accelerate

the electrons transfer from organic substrate to azo bond. The role of RSB as redox mediator was further verified in the continuous flow UASB reactor to enhance the decolorization rate.

References

[1] F.P.V.D. Zee, S. Villaverde, Combined anaerobic-aerobic treatment of azo dyes: a short review of bioreactor studies, Water Res., 39 (2005) 1425–1440.

[2] R.A. Pereira, M.F.R. Pereira, M.M. Alves, L. Pereira, Carbon based materials as novel redox mediators for dye wastewater biodegradation, Appl. Catal. B, Environ., 144 (2014) 713–720.

[3] W. Liu, L. Liu, C. Liu, Y. Hao, H. Yang, B. Yuan, J. Jiang, Methylene blue enhances the anaerobic decolorization and detoxication of aze dye by *Shewanella onediensis* MR-1, Biochem. Eng. J., 110 (2016) 115–124.

[4] F.P.V.D. Zee, R.H.M. Bouwman, D.P.B.T.B. Strik, G. Lettinga, J.A. Field, Application of redox mediators to accelerate the transformation of reactive azo dyes in anaerobic bioreactors, Biotechnol. Bioeng., 75 (2001) 691–701.

[5] F.J. Cervantes, G.E. Jorge, M. Arturo, L.H. Alvarez, A. Sonia, Immobilized humic substances on an anion exchange resin and their role on the redox biotransformation of contaminants, Bioresour. Technol., 102 (2011) 97–100.

[6] J. Chen, W. Hong, T. Huang, L. Zhang, W. Li, Y. Wang, Activated carbon fiber for heterogeneous activation of persulfate: implication for the decolorization of azo dye, Environ. Sci. Pollut. Res. Int., 23 (2016) 18564–18574.

[7] J. Chen, L. Zhang, T. Huang, W. Li, Y. Wang, Z. Wang, Decolorization of azo dye by peroxymonosulfate activated by carbon nanotube: radical versus non-radical mechanism, J. Hazard. Mater., 320 (2016) 571–580.

[8] J. Chen, Y. Wang, C. Fang, T. Huang, C.Y. Wei, Synergistic effect of activated carbon and ultrasonic irradiation on persulfate activation, Desal. Water Treat., 71 (2017) 159–167.

[9] T. Huang, J. Chen, Z. Wang, X. Guo, J.C. Crittenden, Excellent performance of cobalt-impregnated activated carbon in peroxymonosulfate activation for acid orange 7 oxidation, Environ. Sci. Pollut. Res. Int., 24 (2017) 9651–9661.

[10] L.R. Pereira, R. Pereira, M.F. Pereira, M.S. Alves, Carbon Nanotubes as Novel Redox Mediators for Dyed Wastewaters Biodegradation, In: World Congress on Anaerobic Digestion, Santiago De Compostela, 2013, pp. 1–4.

[11] R.A. Pereira, A.F. Salvador, P. Dias, M.F. Pereira, M.M. Alves, L. Pereira, Perspectives on carbon materials as powerful catalysts in continuous anaerobic bioreactors, Water. Res., 101 (2016) 441–447.

[12] R.D. Toro, L.B. Celis, F.J. Cervantes, J.R. Rangel-Mendez, Enhanced microbial decolorization of methyl red with oxidized carbon fiber as redox mediator, J. Hazard. Mater., 260 (2013) 967–974.

[13] M.L. Inyang, B. Gao, Y. Yao, Y. Xue, A. Zimmerman, A. Mosa, P. Pullammanppallil, Y.S. Ok, X. Cao, A review of biochar as a low-cost adsorbent for aqueous heavy metal removal, Crit. Rev. Environ. Sci. Technol., 46 (2016) 406–433.

[14] L.M. Sun, W.Q. Xia, X.F. Zhu, Preparation of activated carbon from modified rice straw and its adsorption of SO_2, Chin. J. Environ. Eng., 11 (2017) 5109–5113 (in Chinese).

[15] B. Xiao, X.F. Sun, R.C. Sun, Chemical, structural, and thermal characterizations of alkali-soluble lignins and hemicelluloses, and cellulose from maize stems, rye straw, and rice straw, Polym. Degrad. Stab., 74 (2001) 307–319.

[16] S.E. Hale, K. Hanley, J. Lehmann, A. Zimmerman, G. Cornelissen, Effects of chemical, biological, and physical aging as well as soil addition on the sorption of pyrene to activated carbon and biochar, Environ. Sci. Technol., 45 (2011) 10445–10453.

[16] C.G. Rocha, D.A. Zaia, R.V. Alfaya, A.A. Alfaya, Use of rice straw as biosorbent for removal of Cu(II), Zn(II), Cd(II) and Hg(II) ions in industrial effluents, J. Hazard. Mater., 166 (2009) 383–388.

[17] A.A. Daifullah, S.M. Yakout, S.A. Elreefy, Adsorption of fluoride in aqueous solutions using $KMnO_4$-modified activated carbon derived from steam pyrolysis of rice straw, J. Hazard. Mater., 147 (2007) 633–643.

[18] C.L. Mantell, Carbon and Graphite Handbook, Wiley, New York, NY, 1968.

[19] S.L. Wang, Y.M. Tzou, Y.H. Lu, G. Sheng, Removal of 3-chlorophenol from water using rice-straw-based carbon, J. Hazard. Mater., 147 (2007) 313–318.

[20] S.Y. Oh, Y.D. Seo, Polymer/biomass-derived biochar for use as a sorbent and electron transfer mediator in environmental applications, Bioresour. Technol., 218 (2016) 77–83.

[21] L. Yu, Y. Yuan, J. Tang, Y. Wang, S. Zhou, Biochar as an electron shuttle for reductive dechlorination of pentachlorophenol by *Geobacter sulfurreducens*, Sci. Rep., 5 (2015) 16221.

[22] H. Benaddi, T.J. Bandosz, J. Jagiello, Surface functionality of activated carbons obtained from chemical activation of wood, Carbon, 38 (2000) 669–674.

[23] R. Demircakan, N. Baccile, M. Antonietti, M.M. Titirici, Carboxylate-rich carbonaceous materials via one-step hydrothermal carbonization of glucose in the presence of acrylic acid, Chem. Mater., 21 (2009) 484–490.

[24] X.H. Guan, G.H. Chen, C. Shang, ATR-FTIR and XPS study on the structure of complexes formed upon the adsorption of simple organic acids on aluminum hydroxide, J. Environ. Sci., 19 (2007) 438–443.

[25] D. Kowalczyk, S. Brzeziński, T. Makowski, W. Fortuniak, Conductive hydrophobic hybrid textiles modified with carbon nanotubes, Appl. Surf. Sci., 357 (2015) 1007–1014.

[26] V. Fierro, V. Tornéfernández, A. Celzard, D. Montané, Influence of the demineralisation on the chemical activation of Kraft lignin with orthophosphoric acid, J. Hazard. Mater., 149 (2007) 126–133.

[27] G.M. Neelgund, A. Oki, Photocatalytic activity of CdS and Ag_2S quantum dots deposited on poly (amidoamine) functionalized carbon nanotubes, Appl. Catal. B, Environ., 10 (2011) 99–107.

[28] L. Pereira, R. Pereira, M.F.R Pereira, Thermal modification of activated carbon surface chemistry improves its capacity as redox mediator for azo dye reduction, J. Hazard. Mater., 183 (2010) 931–939.

[29] H.J. Amezquita-Garcia, E. Razo-Flores, F.J. Cervantes, J.R. Rangel-Mandez, Anchorage of anthraquinone molecules onto activated carbon fibers to enhance the reduction of 4-nitrophenol, J. Chem. Technol. Biotechnol., 90 (2015) 1685–1691.

[30] K. Chizari, A. Deneuve, O. Ersen, F. Ileana, Y. Liu, D. Edouard, I. Janowska, D. Bégin, C. Pham-Huu, Nitrogen-doped carbon nanotubes as a highly active metal-free catalyst for selective oxidation, ChemSusChem, 5 (2012) 102–108.

[31] L. Feng, Y. Yan, Y. Chen, Nitrogen-doped carbon nanotubes as efficient and durable metal-free cathodic catalysts for oxygen reduction in microbial fuel cells, Energy Environ. Sci., 4 (2011) 1892–1899.

[32] H. Fu, D. Zhu, Graphene oxide-facilitated reduction of nitrobenzene in sulfide-containing aqueous solutions, Environ. Sci. Technol., 47 (2013) 4204–4210.

[33] T. Heitmann, C. Blodau, Oxidation and incorporation of hydrogen sulfide by dissolved organic matter, Chem. Geol., 235 (2006) 12–20.

[34] H. Tobias, G. Tobias, B. Julia, B. Christian, Electron transfer of dissolved organic matter and its potential significance for anaerobic respiration in a northern Bog, Global Change Biol., 13 (2007) 1771–1785.

[35] J.J. Orfão, A.I, Silva, J.C. Pereira, S.A. Barata, I.M. Fonseca, P.C. Faria, Adsorption of a reative dye on chemically modified activated carbons--influence of pH, J. Colloid. Interface Sci., 296 (2006) 480–489.

[36] P.C.C. Faria, J.J.M. Órfão, J.L. Figueiredo, M.F.R. Pereira, Adsorption of aromatic compounds from the biodegradation of azo dyes on activated carbon, Appl. Surf. Sci., 254 (2008) 3497–3503.

[37] A.B. Dos, F.J. Cervantes, J.B. Van, Azo dye reduction by thermophilic anaerobic granular sludge, and the impact of the redox mediator anthraquinone-2,6-disulfonate (AQDS) on the reductive biochemical transformation, Appl. Microbiol. Biotechnol., 64 (2004) 62–69.

[38] S.Y. Kim, J.Y. An, B.W. Kim, The effects of reductant and carbon source on the microbial decolorization of azo dyes in an anaerobic sludge process, Dyes Pigm., 76 (2008) 256–263.

[39] A. El-Ghenymy, F. Centellas, J.A. Garrido, R.M. Rodríguez, I. Sirés, P.L. Cabot, Decolorization and mineralization of Orange G azo dye solutions by anodic oxidation with a boron-doped diamond anode in divided and undivided tank reactors, Electrochimica. Acta, 130 (2014) 568–576.

[40] B. Bhushan, A. Halasz, J. Hawari, Effect of iron(III), humic acids and anthraquinone-2,6-disulfonate on biodegradation of cyclic nitramines by *Clostridium* sp. EDB2, J. Appl. Microbiol., 100 (2006) 555–563.

[41] F.P.V.D. Zee, I.A.E. Bisschops, G. Lettinga, Activated carbon as an electron acceptor and redox mediator during the anaerobic biotransformation of azo dyes, Environ. Sci. Technol., 37 (2003) 402–408.

[42] A. Pandey, P. Singh, L. Iyengar, Bacterial decolorization and degradation of azo dyes, Int. Biodeterior. Biodegrad., 59 (2007) 73–84.